ELECTROSPINNING OF ULTRA-THIN POLYMER FIBERS

Raimund Jaeger, Michel M. Bergshoef[†], Cristina Martín i Batlle, Holger
Schönherr, G. Julius Vancso[*]

University of Twente, Chemical Technology, P.O. Box 217,
NL-7500 AE Enschede, The Netherlands.
[†] Centre for Materials Research, University of Twente

Abstract: The electrospinning technique was used to spin ultra-thin fibers from
several polymer/solvent systems. The diameter of the electrospun fibers ranged
from 16 nm to 2 µm. The morphology of these fibers was investigated with an
atomic force microscope (AFM) and an optical microscope. Poly(ethylene oxide)
(PEO) dissolved in water or chloroform was studied in greater detail. PEO fibers
spun from aqueous solution show a "beads on a string" morphology. An AFM
study showed that the surface of these fibers is highly ordered. The "beads on a
string" morphology can be avoided if PEO is spun from solution in chloroform;
the resulting fibers show a lamellar morphology. Polyvinylalcohol (PVA)
dissolved in water and cellulose acetate dissolved in acetone were additional
polymer/solvent systems which were investigated. Furthermore, the
electrospinning process was studied: different experimental lay-outs were tested,
electrostatic fields were simulated, and voltage - current characteristics of the
electrospinning process were recorded.

INTRODUCTION

In the electrospinning process, a high voltage electrostatic field is used to spin thin polymer
fibers from a polymer melt or a polymer solution. The electrostatic spinning technique was
first patented in the late 1930s (ref. 1). Earlier studies of this technique were carried out by
Baumgarten (ref. 2), Larrondo and Manley (ref. 3), and Reneker and co-workers (ref. 4).

Compared to conventional spinning techniques, the electrospinning process can yield very thin fibers. As will be shown later in this work, the thinnest fiber which we were able to observe was a 16 nm wide PEO filament spun from aqueous solution.

Aim of our study is to describe and characterize both the electrospinning process and the electrospun fibers. We used two different experimental lay-outs (a one electrode set-up and a two electrode set-up) for our experiments. Four different polymer/solvent systems were used in our study: (a) poly(ethyleneoxide) (PEO) and water, (b) poly(vinylalcohol) (PVA) and water, (c) PEO and chloroform, and (d) cellulose-acetate and acetone.

EXPERIMENTAL PART

Sample Preparation

PEO (M_w 2,000,000 g/mol) and PVA (M_w 186,000 g/mol) were obtained from Aldrich and were used without further purification. We prepared PEO solutions ranging from 1/2 wt.% to 5 wt.% in distilled water or chloroform. The solutions were gently stirred for 12 h at 50° C (water) or at room temperature (chloroform) in order to obtain homogenous solutions. Aqueous PVA solutions (concentration 8 wt.% and 16 wt.%) were prepared by slowly stirring the polymer for 2-3 hours at 90^oC in distilled water. Cellulose-acetate (obtained from BDH Chemicals Inc., M_η = 40,000 g/mol, degree of acetylation: 2.3 - 2.4) was stirred in acetone for 6 hours at room temperature to prepare 5 wt.% and 8 wt.% solutions.

The Experimental Lay-Out

The spinning solution was placed in a glass capillary (diameter approximately 1 mm). The air pressure above the solution was controlled with an air pump such that a stable drop of the solution was suspended at the tip of the capillary. The air pressure which was applied, could be read from a pressure gauge. A stainless steel pin immersed in the solution was used as electrode. The pin was connected to a Bertan 230-30R high voltage source which can generate dc voltages up to 30 kV. We used a flat metal plate placed below the capillary as grounded counter electrode. The voltage between the electrode and the counter electrode was

displayed on the front panel of the high voltage source. The current between the counter electrode and the ground was measured with a Hewlett Packard HP974A multimeter. The one electrode set-up is displayed in fig. 1(a). The electrostatic field of this configuration was simulated with the Student's Quick Field code (ref. 5) which uses a finite element algorithm. The result of a typical simulation for a given geometry is shown in fig. 1(b).

capillary $\varnothing$ 10 mm
grounded screen: 60 × 5 mm
air-gap: 42 mm
V = 5 kV

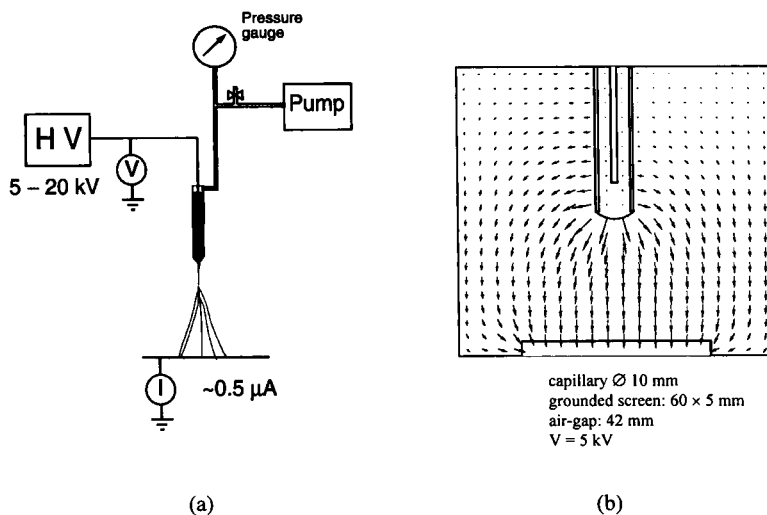(a)   (b)

Fig. 1. Experimental lay-out (a) and electrostatic field (b) of the one-electrode set-up

In addition to the one electrode set-up, we used a two electrode set-up. In this experimental lay-out, an additional ring electrode is placed concentrically between the two electrodes, near the capillary in order to reduce the electrostatic field at the capillary tip. The ring electrode is connected to a second high voltage supply (Bertan 230-20R) which can generate dc voltages up to 20 kV. The two electrode set-up is displayed in fig. 2(a). Fig. 2(b) shows the electrostatic field of this set-up when the ring-electrode and the electrode immersed in the solution are on the same potential. We used similar potentials of both electrodes when we needed to reduce the electrostatic field at the tip of the capillary in order to avoid corona discharges.
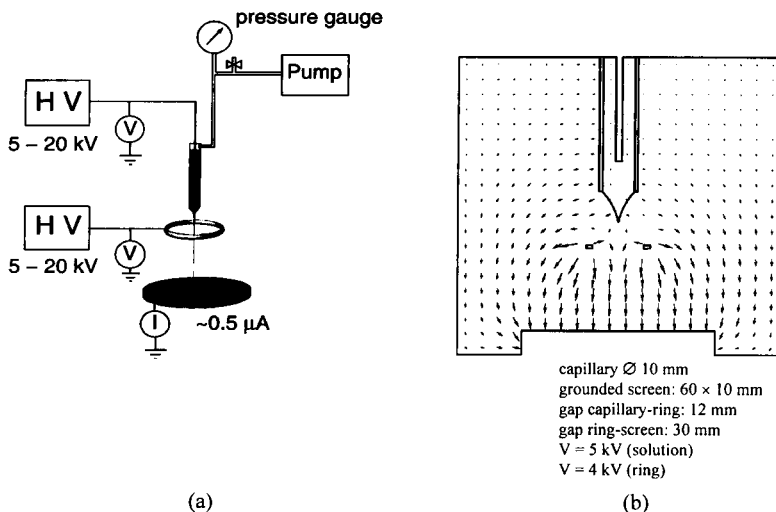
Fig. 2. Experimental lay-out (a) and electrostatic field (b) of the two-electrode set-up

The Electrospinning Process

If an electrical field is applied between the capillary and the counter electrode in the one electrode set-up, the pendant drop at the tip of the capillary is deformed into a conical shape, called the "Taylor cone" (ref. 6) (see fig. 3(a)). At a threshold value of the voltage, the electrostatic forces acting on the surface of the cone overcome the surface tension of the drop, and a jet is ejected from the cone (see fig. 3(b)). After the jet is formed, it remains stable even if the voltage is reduced below the threshold value. Lower voltages result in thinner jets, since less force is used to pull the solution out of the cone (see fig. 3(c)). For certain polymer-solvent systems a "splaying" of the jet into several finer filaments can be observed when the jet is narrowed sufficiently. This narrowing is caused by reduction of the voltage, stretching of the jet in the electrostatic field, or evaporation of the solvent (see fig. 3(d)). Splaying of the jet presumably occurs when an increase of the surface charge density on the jet (due to the reduction of its diameter) leads to a destabilization of the jet. Further reducing the voltage moves the splaying point towards the tip of the capillary.
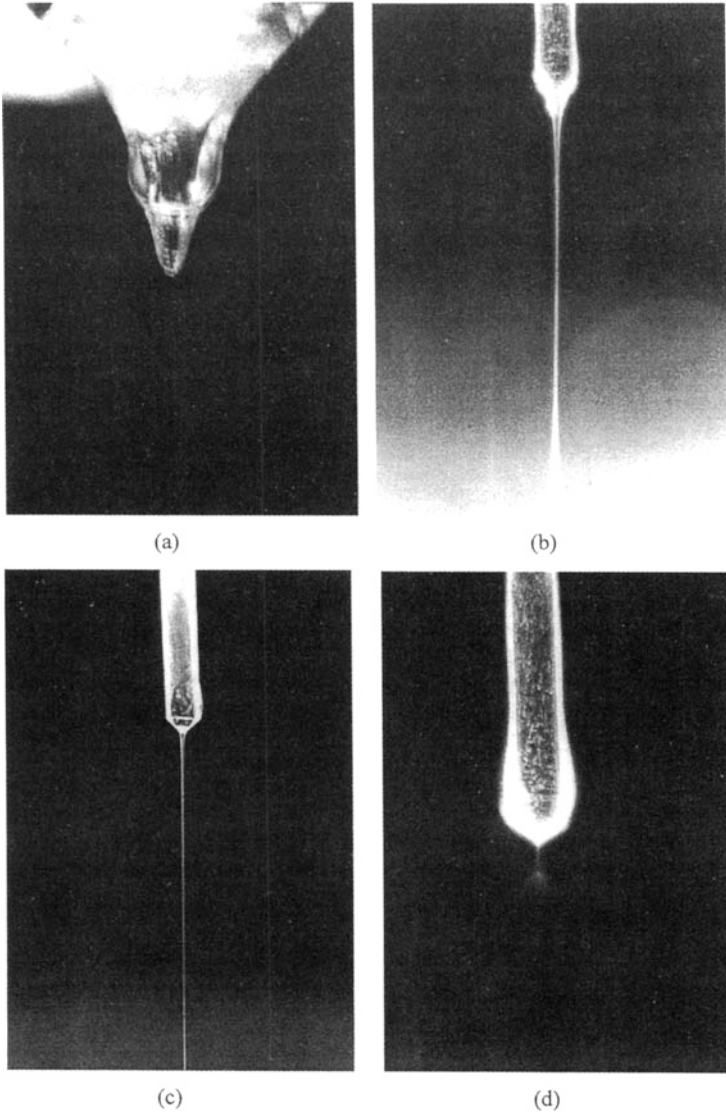
(a)

(b)

(c)

(d)

Fig. 3. Taylor cone (a), initiation (b), stretching (c), and splaying (d) of the jet

Dry fibers can be collected on the counter electrode if the solvent evaporates during the spinning process. This is the case if a volatile solvent (e.g. chloroform or acetone) is used, or if very thin filaments (with a high surface to volume ratio) are created by the splaying of the jet. Electrospun fibers usually form a "non-woven" fabric on the counter electrode.

When the two electrode set-up is used, and when the potential of the steel pin and the ring electrode are similar, the spinning process is not initiated by the electrostatic field, and no Taylor cone is observed. With this set-up, the spinning process starts if a drop of the polymer solution is pulled from the capillary by gravity, and falls through the ring electrode into the electrical field between ring electrode and grounded plate. Apart from the initiation of the jet, the rest of the spinning process is identical to that of the one-electrode set-up. Two advantages of the two electrode set-up are: creation of a field-free space at the tip of the capillary (which is needed for viscous polymer solutions in order to avoid a corona discharge at the tip of the Taylor cone), and the occurrence of a more stable field between ring electrode and counter electrode (the field is not influenced by the sometimes changing shape of the "base" of the jet at the tip of the capillary). Narrowing and splaying of the jet can be easily achieved with the two electrode set-up by increasing the distance between ring electrode and grounded shield (and thus decreasing the electrostatic field) instead of reducing the voltages.

Sample Preparation for AFM and Optical Microscope Studies

We collected electrospun fibers on glass slides for light microscope studies and on microscope cover slides for AFM studies. The slides were placed on the counter electrode and were then covered with fibers. The fibers were examined without any further treatment.

Instruments

The AFM measurements were carried out with a NanoScope III (Digital Instruments, Santa Barbara, CA, USA). AFM scans were carried out in air, using Si_3N_4 cantilevers with a nominal spring constant of 0.38 N/m (NanoTips, Digital Instruments). We used an Olympus BX60 light microscope for optical microscopy. Specific conductivities of the spinning solutions were measured with a Schott CG 854 digital conductometer.

RESULTS AND DISCUSSION

Morphology of Electrospun PEO, PVA, and Cellulose - Acetate Fibers

We were able to electrospin fibers from 1/2 - 3 wt.% aqueous PEO solutions, and 8 wt.% and 16 wt.% aqueous PVA solutions. The electrostatic field pulled droplets from the 4 wt.% and 5 wt.% PEO solutions. These solutions were too viscous to obtain a continuous jet. All PEO and PVA fibers electrospun from aqueous solution showed a "beads on a string" morphology. We observed regularly spaced droplets of similar or alternating sizes along the fibers (see fig. 4(a)). The droplets were typically 1 - 5 μm wide, the diameter of the fibers in between the droplets usually ranged from 200 to 800 nm. The thinnest fiber which we observed was 16 nm wide (see fig. 4(b)). The droplet formation was less pronounced for the more viscous (higher concentrated) solutions. When a fiber is spun from an aqueous solution, it can be regarded as a liquid cylinder which is supported along its axis. In this type of cylinder, liquid flows spontaneously into evenly spaced droplets strung along the core fiber (ref. 6). An alternative explanation for the occurrence of the "beads on a string" morphology is the draw resonance phenomenon, which occurs if fibers are drawn to a high draw ratio (ref. 7). The draw resonance phenomenon (i.e. the formation of droplets) proceeds more slowly for more viscous solutions. This is in agreement with our observations on the electrospinning of more viscous solutions. However, a high level of orientation in the bulk of the fibers has not yet been proven.
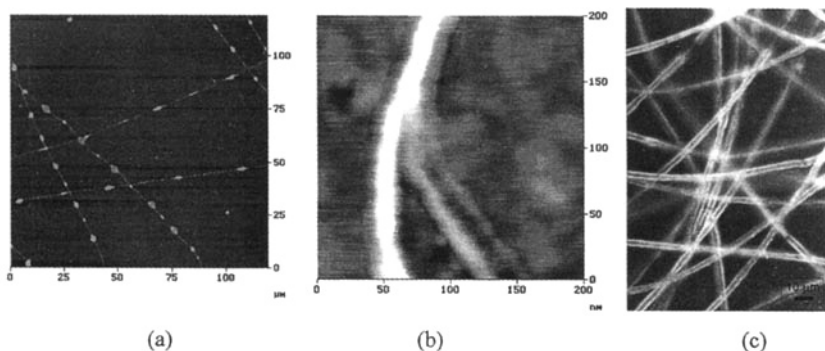

(a)   (b)   (c)

Fig. 4. (a) "Beads on a string" morphology of electrospun PEO fibers. (b) AFM nanograph of a 16 nm wide PEO fiber. (c) PEO fibers spun from solution in chloroform

The surface of electrospun PEO fibers is highly ordered. We obtained AFM nanographs of the surface topology of PEO fibers electrospun from a 1 wt.% solution which showed the packing of PEO chains (ref. 8). The chain direction and fiber direction were predominantly parallel.

Droplet formation was avoided when a PEO/chloroform solution was spun. We obtained 1 - 2 μm wide fibers of uniform thickness (see fig. 4(c)). During the spinning process, the solvent evaporated before splaying of the jet or droplet formation could set in. AFM images of the surface of the fibers showed lamellar structures. An oriented surface layer (as observed for the fibers spun from aqueous solution) could not be achieved before the evaporation of the solvent.

Cellulose - acetate spun from solution in acetone yielded short fibers which were thinner than 1 μm. These fibers also showed the "beads on a string" morphology.

Current - Voltage Characteristics for the Electrospinning Process of PEO/Water

Current - voltage curves for different distances between capillary and grounded shield (i.e. different jet lengths) are shown in fig. 5. The curves were recorded while the pressure above the liquid in the capillary and the height of the liquid column in the capillary were kept approximately constant. The resistance of the jet depends on its geometry. The resistance decreases with increasing voltage (indicative of a larger diameter) and with decreasing distance between capillary and counter electrode.

The diameter of the jet was measured with laser light diffraction (ref. 9, 10). Preliminary results (obtained in a given experiment) show that the diameter of the jet decreases to 19 μm after travelling one centimeter, 11 μm after travelling 2 cm, and 9 μm after travelling 3.5 cm from the orifice. The diameter of the jet is (at constant distance to the orifice and constant voltage) sensitive to variations of the air pressure above the spinning solution.

In addition, we carried out measurements of the current - voltage curves of conducting PEO/water/KCl solutions, where we controlled the conductivity of the spinning solutions with the KCl content. We were able to electrospin solutions when their conductivity was below 1500 μS cm^{-1}. The high voltage was short-circuited for higher conductivities when the

jet reached the counter electrode, and thus no continuous spinning process could be achieved. For conductivities in the range of 1000 - 1500 μS cm^{-1}, we observed a heating up of the jet by the electrical current: the jet began to steam.
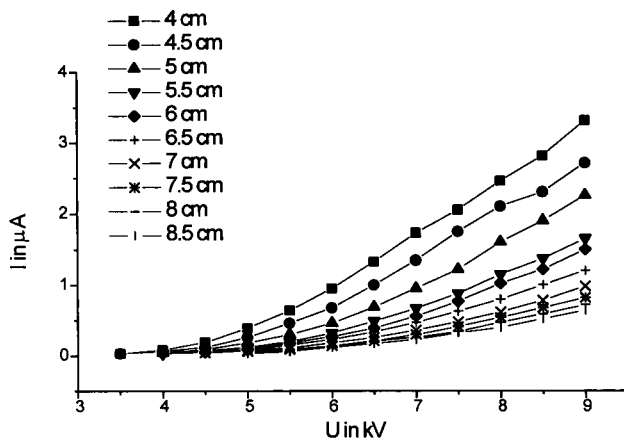

Fig. 5. Current - voltage curves of the electrospinning process of 2 wt.% aqueous PEO solution for different jet lengths

Possible Applications of Electrospun Fibers

Typical applications of electrospun fibers are those where a high surface to volume ratio is important. Electrospun fibers are therefore often used as filter materials (ref. 11). In fig. 6(a) a layer of PEO fibers is shown which was electrospun onto a metal mesh. Another possible application of electrospun fibers are fiber-reinforced materials. The high interfacial area can lead to an improved performance of a composite. Fig. 6(b) shows an oriented layer of electrospun fibers which could be used in mono-directional composites. The PEO fibers shown in fig. 6 were spun with the two electrode set-up.
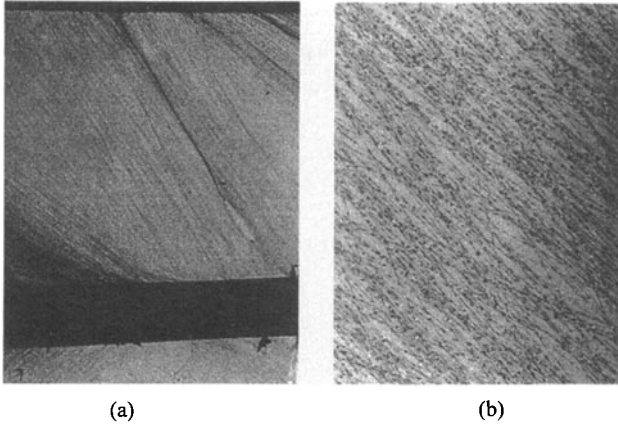
(a)   (b)

Fig. 6. PEO fibers electrospun onto a metal mesh (a) and an oriented layer of electrospun PEO fibers (b)

REFERENCES

(1)   A. Formhals, U.S. Patent 2,116,942 (1938)
(2)   P. K. Baumgarten, *J. Coll. Interface Sci.* **36**, 71, (1971)
(3)   (a) L. Larrondo, R. S. J. Manley, *J. Polym. Sci., Polym. Phys. Ed.* **19**, 909, (1981),
        (b) L. Larrondo, R. S. J. Manley, *J. Polym. Sci., Polym. Phys. Ed.* **19**, 921, (1981),
        (c) L. Larrondo, R. S. J. Manley, *J. Polym. Sci., Polym. Phys. Ed.* **19**, 933, (1981)
(4)   (a) J. Doshi, G. Srinivasan, D. H. Reneker, *Polym. News* **20**, 206, (1995), (b) J. Doshi,
        D. H. Reneker *J. Electrost.* **35**, 151, (1995), (c) G. Srinivasan, J. Doshi, D. H. Reneker
        Polym. International **36**, 195, (1995), (d) D. H. Reneker, I. Chun, *Nanotechnology* **7**,
        216, (1996)
(5)   Student's Quick Field ™, Tera Analysis Co., Tarzana, CA, US.
(6)   J.W.S. Rayleigh, *Philos. Mag.* **34**, 145, (1892)
(7)   D. W. Bousfield, R. Keunings, G. Marrucci, M. M. Denn *J. Non-Newtonian Fluid
        Mech.* **21**, 79. (1986)
(8)   R. Jaeger, H. Schönherr, G. J. Vancso *Macromolecules* **29**, 7634, (1996)
(9)   A. J. Perry, B. Ineichen, B. Eliasson *J. Mat. Sci.* **9**, 1373, (1974)
(10)   C. Martin, Internal report, University Twente, (1997)
(11)   D. Groitzsch, E. Fahrbach, German Patent DE 3437183 A1 860417 (1986)